



This is a repository copy of *Study of mass transfer correlations for rotating packed bed columns in the context of solvent-based carbon capture*.

White Rose Research Online URL for this paper:
<http://eprints.whiterose.ac.uk/154476/>

Version: Accepted Version

Article:

Oko, E. orcid.org/0000-0001-9221-680X, Wang, M. orcid.org/0000-0001-9752-270X and Ramshaw, C. (2019) Study of mass transfer correlations for rotating packed bed columns in the context of solvent-based carbon capture. *International Journal of Greenhouse Gas Control*, 91. 102831. ISSN 1750-5836

<https://doi.org/10.1016/j.ijggc.2019.102831>

Article available under the terms of the CC-BY-NC-ND licence
(<https://creativecommons.org/licenses/by-nc-nd/4.0/>).

Reuse

This article is distributed under the terms of the Creative Commons Attribution-NonCommercial-NoDerivs (CC BY-NC-ND) licence. This licence only allows you to download this work and share it with others as long as you credit the authors, but you can't change the article in any way or use it commercially. More information and the full terms of the licence here: <https://creativecommons.org/licenses/>

Takedown

If you consider content in White Rose Research Online to be in breach of UK law, please notify us by emailing eprints@whiterose.ac.uk including the URL of the record and the reason for the withdrawal request.



eprints@whiterose.ac.uk
<https://eprints.whiterose.ac.uk/>

Study of mass transfer correlations for rotating packed bed columns in the context of solvent-based carbon capture

Eni Oko, Meihong Wang*, Colin Ramshaw

Department of Chemical and Biological Engineering, University of Sheffield, S1 3JD, UK

*Corresponding Author: Tel.: +44 1114 222 7160. E-mail address: Meihong.Wang@sheffield.ac.uk

Abstract

The application of rotating packed beds (RPBs) in solvent-based carbon capture processes, will greatly reduce the physical footprint, capital and operating cost of the process. However, in designing RPBs, correlations for predicting mass transfer parameters are generally limited in literature and their prediction accuracies have not been demonstrated independently. In this paper, an RPB absorber model was developed in gPROMS ModelBuilder® and used to test and compare different correlations for predicting the effective interfacial area, liquid and gas film mass transfer coefficients. Our results showed that the modified packed column mass transfer correlations where the “g” term (i.e. gravitational acceleration) replaced with “rw²” (i.e. centrifugal acceleration) commonly used in literature for RPBs generally give poor predictions compared to using correlations developed specifically for RPBs. Also, the Tung and Mah correlation has better predictive accuracy for the liquid film mass transfer coefficient in RPBs than more complex correlations. Finally, a set of new data for the gas film mass transfer coefficient for RPBs were also derived from overall volumetric mass transfer coefficient ($K_G a$) experimental data from literature. This is the first report of gas film mass transfer data for RPBs. The results in this paper will guide researchers in selecting suitable correlations for predicting mass transfer parameters in RPBs.

Keywords: solvent-based CO₂ capture; rotating packed bed; effective interfacial area; liquid film mass transfer coefficient; gas film mass transfer coefficient

Nomenclature

a	Effective interfacial area of packing per unit volume (m ² /m ³)
a_t	Total area of packing per unit volume (m ² /m ³)
A	Tangential section area (m ²) = $2\pi rZ$
c, d	Packing parameters for Luo et al. (2012a) correlation ($c = 3.5$ mm, $d = 1.0$ mm)
C_p^L	Liquid specific heat capacity (J/kg K)
d_h	Hydraulic diameter (m) = $4\epsilon/a_t$
d_p	Effective diameter of packing (m) = $6(1 - \epsilon)/a_t$
D_L	Liquid diffusivity (m ² /s)
D_G	Gas diffusivity (m ² /s)
E	Enhancement factor
G^m	Gas molar flowrate (kmol/s)
h_G	Gas phase specific molar enthalpy (J/kmol)
h_L	Liquid phase specific molar enthalpy (J/kmol)
$h_{g/l}$	Interfacial heat transfer coefficient (W/m ² K)
H	Henry constant
ΔH_r	Heat of absorption (J/kmol)
ΔH_{vap}	Heat of vaporisation of H ₂ O (J/kmol)
k_G	Gas film mass transfer coefficient (m/s)
$K_G a$	Overall volumetric mass transfer coefficient based on gas side (1/s)
k_L	Liquid film mass transfer coefficient (m/s)
$K_L a$	Overall volumetric mass transfer coefficient based on liquid side (1/s)
k_{app}	Apparent reaction rate constant
L^m	Liquid molar flowrate (kmol/s)
L_m^*	Liquid mass flowrate per unit tangential section area (kg/m ² s)
N_i	Component molar fluxes (kmol/m ² s)
Q_L	Liquid volumetric flowrate (m ³ /s)
Q_V	Gas volumetric flowrate (m ³ /s)
r	Radius (m)

r_i	Inner radius of the packed bed (m)
r_o	Outer radius of the packed bed (m)
r_s	Radius of the stationary housing (m)
RPM	Revolutions per minute
T_g, T_l	Gas and liquid side temperature (K)
u_L	Liquid velocity (m/s)
V_G	Parameter for Chen et al. (2011) gas film model = $1 - 0.9 \frac{V_o}{V_t}$
V_L	Parameter for Chen et al. (2006) liquid film model = $1 - 0.93 \frac{V_o}{V_t} - 1.13 \frac{V_i}{V_t}$
V_i	Volume inside the inner radius of the bed (m^3) = $\pi r_i^2 Z$
V_m^*	Gas mass flowrate per unit tangential section area ($kg/m^2 s$)
V_O	Volume between the outer radius of the bed and the stationary housing (m^3) = $\pi(r_s^2 - r_o^2)Z$
V_t	Total volume of the RPB (m^3) = $\pi r_s^2 Z$
x_i	Component molar fraction in liquid phase
y_i	Component molar fraction in gas phase
Z	Height of the rotor (m)

Greek Letters

σ_c	Critical surface tension for packing material (= 0.075 N/m)
σ_L	Liquid surface tension (N/m)
ε	Packing porosity (m^3/m^3)
ρ_G	Gas density (kg/m^3)
ρ_L	Liquid density (kg/m^3)
λ_L	Liquid thermal conductivity (W/m K)
μ_G	Gas dynamic viscosity (Pa s)
μ_L	Liquid dynamic viscosity (Pa s)
ω	Rotating speed (rad/s)

22 1. Introduction

23 1.1 Background

24 The gas-liquid packed columns are an important unit operation in natural gas treating and solvent-based CO₂
 25 capture processes where they are used for absorption and desorption. The packed columns in these processes are
 26 large in size, contributing significantly to physical footprint, capital and operating costs (Lawal et al., 2012;
 27 IEAGHG, 2013; Oko, 2015). An engineering estimate showed that absorbers in a solvent-based CO₂ capture
 28 (PCC) plant using monoethanolamine (MEA) solvent for capturing CO₂ from a 500 MWe coal-fired subcritical
 29 power plant will have diameters up to 25 m and packing height over 27 m (Oko, 2015). This will significantly
 30 increase the land use per MWe when coal and gas fired power plants are integrated with PCC plants (Florin and
 31 Fennel, n.d.).

32 Through process intensification (PI), wherein the packed columns are replaced with rotating packed beds (RPBs),
 33 the physical footprint of the process could be reduced significantly (Joel et al., 2014; Thiels et al., 2016).
 34 Theoretical investigations by Agarwal et al. (2010) and Joel et al. (2014) showed about 10-12 times reduction in
 35 the absorber size when it is replaced with an RPB. The HiGee Environment and Energy Technologies Inc. USA
 36 also reported about 10 times size reduction in a commercial scale RPB installed to replace a packed column at the
 37 Fujian Refining and Petrochemical Company Ltd, China (HiGee, 2014). The reported size reductions are
 38 consistent with predictions about RPBs in earlier investigations by Chambers and Wall (1954) and Ramshaw and
 39 Mallinson (1981).

40 1.2 Principle of RPB and problem statement

41 The RPB generally includes a cased annular packed bed (rotor), made of packing materials such as glass bead
 42 (Munjal et al., 1989a&b), corrugated disk (Chen et al., 1997; Chen et al., 1999), wire mesh (Luo et al., 2012),
 43 expamet (Jassim et al., 2007), blade packing with static baffles (Tsai and Chen, 2015), nickel foam (Chu et al.,
 44 2015) etc. and mounted on a rotating shaft (Fig. 1). The gas and liquid phases enter the RPB through the outer and

85 This study provides an extensive review and comparison of all published correlations for estimating different mass
 86 transfer parameters for RPBs, namely effective interfacial area, liquid and gas film mass transfer coefficients. As
 87 noted in Section 1.3, related study had been reported by Joel et al. (2014) and Kang et al. (2014). However, neither
 88 study included comparisons for gas film mass transfer coefficient and they considered the correlations in sets (See
 89 Section 1.3) and validated overall predictions of their RPB model and not specific predictions of the mass transfer
 90 parameters. This study will therefore address the following gaps identified from existing studies:

- 91 a. No information on performance of correlations for predicting gas film mass transfer coefficients for RPBs
 92 b. No specific performance comparison of different mass transfer correlations for RPBs.
 93 c. No data for the gas film mass transfer coefficient for RPBs. An assessment comparing liquid and gas film
 94 resistances to mass transfer for CO₂ absorption in different MEA concentrations in an RPB absorber (Table
 95 1) show that the gas film resistance could be over 10% of the overall resistance and cannot be ignored.
 96 Obtaining data for the gas film mass transfer coefficient is therefore essential. The gas film mass transfer
 97 coefficient data were derived from overall volumetric mass transfer coefficient ($K_G a$) experimental data from
 98 the literature.

99 Table 1: Liquid and gas film resistances for an RPB absorber with MEA solvent*

MEA (wt%)	Liquid film resistance (Pa m ² s/mol)	Gas film resistance (Pa m ² s/mol)
55	240490.2	23265.93
75	172447.4	25305.32

100 *The liquid and gas film resistances have been obtained using conditions from Jassim et al. (2007) and reaction data from Ying and Eimer
 101 (2013). The liquid and gas film mass transfer coefficients were respectively obtained using Tung and Mah (1985) and Chen (2011).

102 2. Methodology – model development

103 The mass transfer parameters for the RPB derived from experimental measurements are reported in literature. In
 104 this study, selected RPB absorber rigs from literature used for deriving different mass transfer parameters are
 105 represented using models derived from first principle. The details of the selected rigs are given in Section 3
 106 (effective interfacial area), Section 4 (liquid film mass transfer coefficient) and Section 5 (gas film mass transfer
 107 coefficient). In the RPB absorber model, different mass transfer correlations (See Sections 3, 4 & 5) are used to
 108 predict mass transfer parameters. The predicted values for different correlations are then compared to their
 109 counterpart derived from experimental measurements for the selected case in the literature. The RPB absorber
 110 model, developed using gPROMS ModelBuilder®, are represented using Equations 1-9. The thermo-physical
 111 properties are obtained using a combination of the electrolyte Non-Random Two-Liquid (elecNRTL) model in
 112 Aspen Plus® and data obtained from the literature. The elecNRTL model is accessed from gPROMS
 113 ModelBuilder® platform through the CAPE-OPEN interface. The model has been validated for CO₂ absorption in
 114 MEA cases and presented in Oko et al. (2018). The following assumptions have been made in developing the
 115 model:

- 116 ▪ Steady state conditions.
- 117 ▪ One-dimensional differential mass and energy balances for liquid and gas phases
- 118 ▪ Heat losses are neglected
- 119 ▪ Heat and mass transfer are described using the two-film theory
- 120 ▪ Reactions (where applicable) are accounted for using an enhancement factor in the overall mass transfer
 121 coefficient

122 Material balance

$$123 \text{ Gas phase: } 0 = \frac{1}{2\pi r Z} \frac{\partial(G^m y_i)}{\partial r} - a N_i \quad (1)$$

$$124 \text{ Liquid phase: } 0 = -\frac{1}{2\pi r Z} \frac{\partial(L^m x_i)}{\partial r} + a N_i \quad (2)$$

125 Energy balance

$$126 \text{ Gas phase: } 0 = \frac{1}{2\pi r Z} \frac{\partial(G^m h_G)}{\partial r} - a h_{g/l} (T_l - T_g) \quad (3)$$

127

$$128 \quad \text{Liquid phase: } 0 = -\frac{1}{2\pi r z} \frac{\partial(L^m h_L)}{\partial r} + a(h_{g/l}(T_l - T_g) - \Delta H_r N_{CO_2} - \Delta H_{vap} N_{H_2O}) \quad (4)$$

129 The molar fluxes for molecular components are obtained as follows based on the two-film theory:

$$130 \quad N_i = K_{G,i}(P_{g,i} - P_i^{eq}) \quad (5)$$

131 The overall mass transfer coefficient ($K_{G,i}$) comprise of mass transfer resistances on both the gas and liquid film
 132 (Eqn. 6). $P_{g,i}$ and P_i^{eq} are respectively gas phase component partial pressure and component equilibrium partial
 133 pressure in the liquid phase.

$$134 \quad K_{G,i} = \frac{1}{\left(\frac{RT_g}{k_{G,i}}\right) + \left(\frac{H}{k_{L,i}E}\right)} \quad (6)$$

135 The enhancement factor (E) is used to account for the reactions in reactive cases. The enhancement factor (E) is
 136 obtained on the basis of a pseudo first-order reaction regime as given in Eqn 7.

$$137 \quad E = \frac{\sqrt{k_{app} D_{L,CO_2}}}{k_{L,CO_2}} \quad (7)$$

138 Finally, the interfacial heat transfer coefficient ($h_{g/l}$) is obtained based on the Chilton-Colburn analogy:

$$139 \quad h_{g/l} = k_L \rho_L C_p^L \left(\frac{\lambda_L}{\rho_L C_p^L D_L} \right)^{\frac{2}{3}} \quad (8)$$

140 3. Case 1: Effective interfacial area

141 3.1 Experimental data and correlations

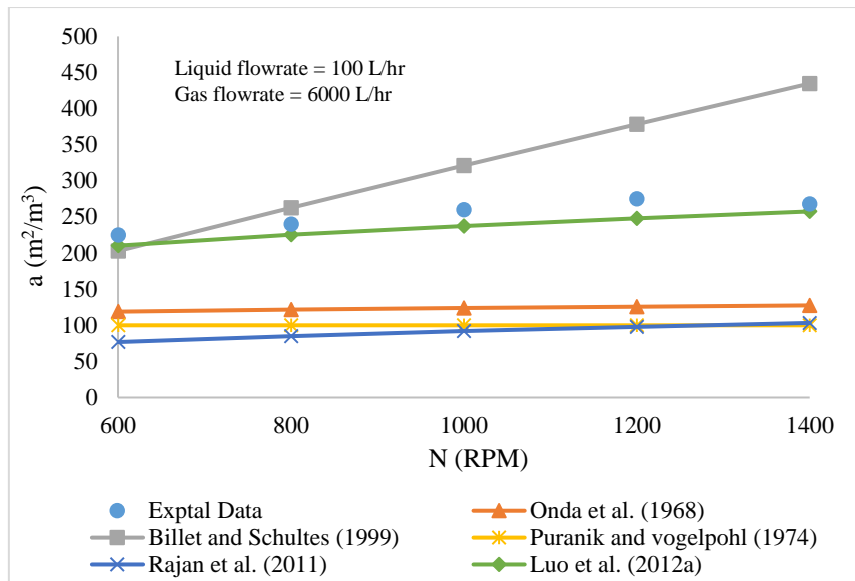
142 In the literature, effective interfacial area data for RPB have been derived from measurements of CO₂ absorption
 143 in NaOH solutions (Munjal et al., 1989b; Chen et al., 1997; Chen et al., 1999; Rajan et al., 2011; Yang et al.,
 144 2011; Luo et al., 2012a; Guo et al., 2014; Chu et al., 2015; Liu et al., 2015; Tsai and Chen, 2015; Luo et al., 2017)
 145 based on the approach proposed by Sharma and Danckwerts (1970). The reported data are mainly packing
 146 effective interfacial area; a few studies (Yang et al., 2011; Guo et al., 2014; Luo et al., 2017) reported the effective
 147 interfacial area for the different mass transfer zones, namely the packing, cavity and the end zones. It was found
 148 that the packing effective interfacial area make up more than half of the total effective interfacial area (Yang et al.,
 149 2011). Recent studies have also investigated the effective interfacial area for novel packing designs, namely blade
 150 packing RPB with static baffles (Tsai and Chen, 2015), nickel foam packing (Chu et al., 2015) and structured wire
 151 mesh packing (Luo et al., 2017). Changes in the packing design was shown to have significant impact on the
 152 effective interfacial area (Tsai and Chen, 2015). The data from Luo et al. (2012a) was selected for this work. The
 153 Luo et al. (2012a) experiments comprised of a 1M NaOH solution as the liquid phase and a mixed CO₂ and N₂
 154 gas with approximately 10 mol% of CO₂ as the gas phase. The data is preferred to the data from other sources for
 155 the following reasons:

- 156 ▪ The RPB used for obtaining the measurements (Table 2 Specification of RPB from is equipped with wire
 157 mesh packing. Wire mesh packings are proven to be very suitable for RPBs due to their better mass
 158 transfer performance and rigidity (Chen et al. 2006). Munjal et al. (1989b) data was obtained from an
 159 RPB with glass bead packing. Chen et al. (1997) and Chen et al. (1999) data were obtained from an
 160 RPB with corrugated disk packings.
- 161 ▪ The packing is a traditional RPB design, wherein the packings are loaded uniformly across the radial
 162 depth of the RPB without gaps in-between packing rings, so called unsplit packing configuration (Figure
 163 2). The packing is held between two disks and rotated by a single motor. Rajan et al. (2011) and Liu et
 164 al. (2015) on the other hand are based on split packing configuration, a relatively new packing design for
 165 RPBs. The split packing configuration comprise of alternate annular packing rings attached to two
 166 separate disks with a small radial gap between adjacent rings when the two disks are brought together
 167 (Figure 3) with the disks rotated by two separate motors counter-currently or co-currently.

193 Billets and Schultes (1999) correlation (i.e. with “g” term replaced by “ $r\omega^2$ ” term) although the deviation becomes
 194 increasingly large at high rotating speed. The predictions of Puranik and Vogelpohl (1974) correlation show nearly
 195 50% deviation. Comparing the predictions of Puranik and Vogelpohl (1974) with others at different rotating speed
 196 also highlight the impact of centrifugal acceleration. Although, Puranik and Vogelpohl (1974) correlation has
 197 been used successfully for packed columns, they clearly show poor prediction accuracy for RPBs. This partly
 198 because the correlation that do not have an acceleration term. Finally, the performance of Rajan et al. (2011)
 199 correlation which is developed for RPB was a bit surprising. The predictions deviated by nearly 50%. The Rajan
 200 et al. (2011) correlation is based on split packing configuration and this is viewed as a major reason for the large
 201 error when the correlation is used for predicting the effective interfacial area for unsplit packing configuration in
 202 this study. It is recommended that the Rajan et al. (2011) correlation be used for split packing configuration cases
 203 only as it clearly underperforms for unsplit packing configuration case as shown in this study.

204 Table 3 Correlations for calculating effective interfacial area in RPB

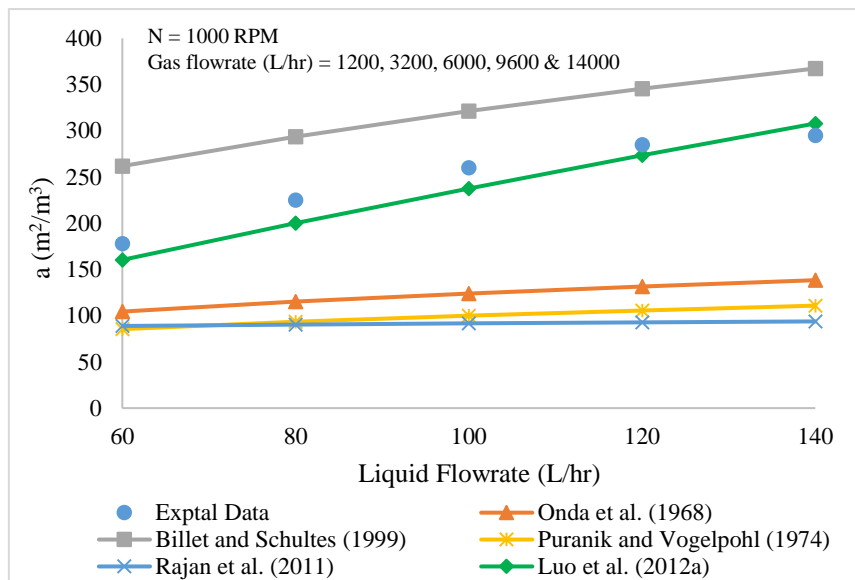
Correlations	Source	Comment
$\frac{a}{a_t} = 1 - \exp \left[-1.45 \left(\frac{\sigma_c}{\sigma_L} \right)^{0.75} \left(\frac{L_m^*}{a_t \mu_L} \right)^{0.1} \left(\frac{a_t L_m^{2*}}{r \omega^2 \rho_L^2} \right)^{-0.05} \left(\frac{L_m^{2*}}{\sigma_L \rho_L a_t} \right)^{0.2} \right]$	Onda et al. (1968)	These correlations have been modified for RPB by replacing the “g” term with “ $r\omega^2$ ” term.
$\frac{a}{a_t} = 1.5 (a_t d_h)^{-0.5} \left(\frac{\rho_L u_L d_h}{\mu_L} \right)^{-0.2} \left(\frac{\rho_L u_L^2 d_h}{\sigma_L} \right)^{0.75} \left(\frac{u_L^2}{r \omega^2 d_h} \right)^{-0.45}$	Billets and Schultes (1999)	
$\frac{a}{a_t} = 1.045 \left(\frac{L_m^*}{a_t \mu_L} \right)^{0.041} \left(\frac{L_m^{2*}}{\sigma_L \rho_L a_t} \right)^{0.133} \left(\frac{\sigma_c}{\sigma_L} \right)^{0.182}$	Puranik and Vogelpohl (1974)	This do not have a “g” term. It was selected to know if good predictions are possible in RPB without explicitly accounting for acceleration.
$\frac{a}{a_t} = 54999 \left(\frac{\rho_L d_p u_L}{\mu_L} \right)^{-2.2186} \left(\frac{u_L^2}{r \omega^2 d_p} \right)^{-0.1748} \left(\frac{\rho_L d_p u_L^2}{\sigma_L} \right)^{1.3160}$	Rajan et al. (2011)	These correlations are developed for RPB. Rajan et al. (2011) is based on split packing type RPB rotated by two separate motors.
$\frac{a}{a_t} = 66510 \left(\frac{\rho_L d_p u_L}{\mu_L} \right)^{-1.41} \left(\frac{u_L^2}{r \omega^2 d_p} \right)^{-0.12} \left(\frac{\rho_L d_p u_L^2}{\sigma_L} \right)^{1.21} \left(\frac{c^2}{(c+d)^2} \right)^{-0.74}$	Luo et al. (2012a)	



206

207

Figure 4 Predictions of different correlations for effective interfacial area at different RPM



208

209

Figure 5 Predictions of different correlations for effective interfacial area at different liquid flowrate

210 4. Case 2: Liquid film mass transfer coefficient (k_L)

211 4.1 Experimental data and correlation

212 The study of liquid side mass transfer in RPBs is reported widely in literature, although it is the overall volumetric
 213 mass transfer coefficients ($K_L a$) and the volumetric liquid side mass transfer coefficients ($k_L a$) rather than the
 214 liquid film mass transfer coefficient (i.e. k_L) that are generally determined from experiments due to the difficulties
 215 in estimating the effective interfacial area in RPBs (Chen et al., 2005a; Chen et al., 2005b; Chen et al., 2006; Lin
 216 and Liu, 2007). The only existing liquid film mass transfer coefficient data is reported by Luo et al. (2012b) and
 217 the experimental data has been selected for independently verifying different correlations for predicting liquid
 218 film mass transfer coefficients in this study. The data were derived from measurements of CO_2 absorption in
 219 NaOH solutions based on the approach proposed by Sharma and Danckwerts (1970). The authors assumed a
 220 pseudo-first order reaction kinetics regime with mass transfer controlled by the liquid phase resistance. The liquid
 221 and gas phase were respectively 0.05 M NaOH solution and a mixed gas of CO_2 and N_2 with about 2 mol % of
 222 CO_2 . A summary of the RPB parameters from Luo et al. (2012b) is given in Table 4.

Table 4 Specification of RPB from Luo et al. (2012b)

Dimensions (mm)				Packing		
r_i	r_o	r_s	Z	Type	a_t	ε
78	153	248	50	Wire mesh	500	0.96

224 Presently, only five correlations (Table 5) for predicting the liquid film mass transfer coefficient have been
 225 published in literature (Tung and Mah, 1985; Munjal et al., 1989a; Chen et al., 2005a; Chen et al., 2005b; Chen
 226 et al., 2006); an elaborate model based on surface renewal theory has also been proposed by Ding et al. (2000).
 227 The reported correlations were developed from theoretical principle based on penetration theory (Tung and Mah,
 228 1985; Munjal et al., 1989a) and the film theory (Chen et al., 2005a; Chen et al., 2005b; Chen et al., 2006).

229 In this study, the performance of these five correlations, the summary of which are given in Table 5 Correlations
 230 for calculating liquid film mass transfer coefficient in RPB5, are evaluated. The modified Onda et al. (1968) was
 231 selected to demonstrate their performance for predicting k_L for RPBs. The Tung and Mah (1985) correlation is
 232 simpler and requires fewer parameters compared to others. The Chen et al. (2006) correlation on the other hand
 233 is very elaborate, accounting for both the packing geometry and mass transfer in the end zones otherwise called
 234 the end effect phenomenon.

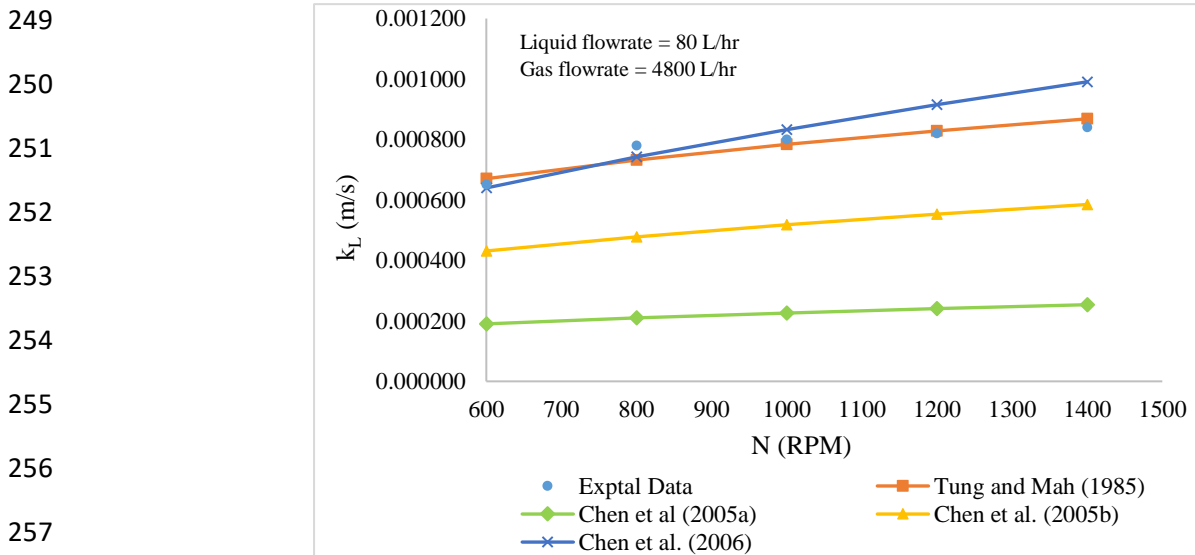
235 Table 5 Correlations for calculating liquid film mass transfer coefficient in RPB

Correlations	Source	Comment
$k_L \left(\frac{\rho_L}{\mu_L r \omega^2} \right)^{\frac{1}{3}} = 0.0051 \left(\frac{L_m^*}{a \mu_L} \right)^{\frac{2}{3}} \left(\frac{\mu_L}{\rho_L D_L} \right)^{\frac{1}{2}} (a_t d_p)^{0.4}$	Onda et al. (1968)	Modified for RPB by replacing the “g” term with “ $r\omega^2$ ” term.
$\frac{k_L d_p}{D_L} = 0.918 \left(\frac{\mu_L}{D_L \rho_L} \right)^{\frac{1}{2}} \left(\frac{L_m^*}{\mu_L a_t} \right)^{\frac{1}{3}} \left(\frac{a_t}{a} \right)^{\frac{1}{3}} \left(\frac{d_p^3 \rho_L^2 r \omega^2}{\mu_L^2} \right)^{\frac{1}{6}}$	Tung and Mah (1985)	The correlations are developed for predicting k_L in RPBs. They do not account for end effect and packing type
$k_L = 2.6 \frac{\pi L_m^*}{2 a \rho_L X} \left(\frac{\mu_L}{D_L \rho_L} \right)^{\frac{1}{2}} \left(\frac{2 \pi L_m^*}{\mu_L a_t} \right)^{\frac{2}{3}} \left(\frac{X^3 \rho_L^2 r \omega^2}{\mu_L^2} \right)^{\frac{1}{6}}$	Munjal et al. (1989a)	
$\frac{k_L a d_p}{D_L a_t} = 0.9 \left(\frac{\mu_L}{D_L \rho_L} \right)^{0.5} \left(\frac{L_m^*}{\mu_L a_t} \right)^{0.24} \left(\frac{d_p^3 \rho_L^2 r \omega^2}{\mu_L^2} \right)^{0.29} \left(\frac{L_m^*}{\sigma_L \rho_L a_t} \right)^{0.29}$	Chen et al. (2005a)	The correlations are developed for predicting $k_L a$ in RPBs. Chen et al. (2006) accounts for both end effect and packing type
$\frac{k_L a d_p}{D_L a_t} V_L = 0.65 \left(\frac{\mu_L}{D_L \rho_L} \right)^{0.5} \left(\frac{L_m^*}{\mu_L a_t} \right)^{0.17} \left(\frac{d_p^3 \rho_L^2 r \omega^2}{\mu_L^2} \right)^{0.3} \left(\frac{L_m^*}{\sigma_L \rho_L a_t} \right)^{0.3}$	Chen et al. (2005b)	
$\frac{k_L a d_p}{D_L a_t} V_L = 0.35 \left(\frac{\mu_L}{D_L \rho_L} \right)^{0.5} \left(\frac{L_m^*}{\mu_L a_t} \right)^{0.17} \left(\frac{d_p^3 \rho_L^2 r \omega^2}{\mu_L^2} \right)^{0.3} \left(\frac{L_m^*}{\sigma_L \rho_L a_t} \right)^{0.3} \left(\frac{a_t}{a_p} \right)^{-0.5} \left(\frac{\sigma_c}{\sigma_L} \right)^{0.14}$	Chen et al. (2006)	

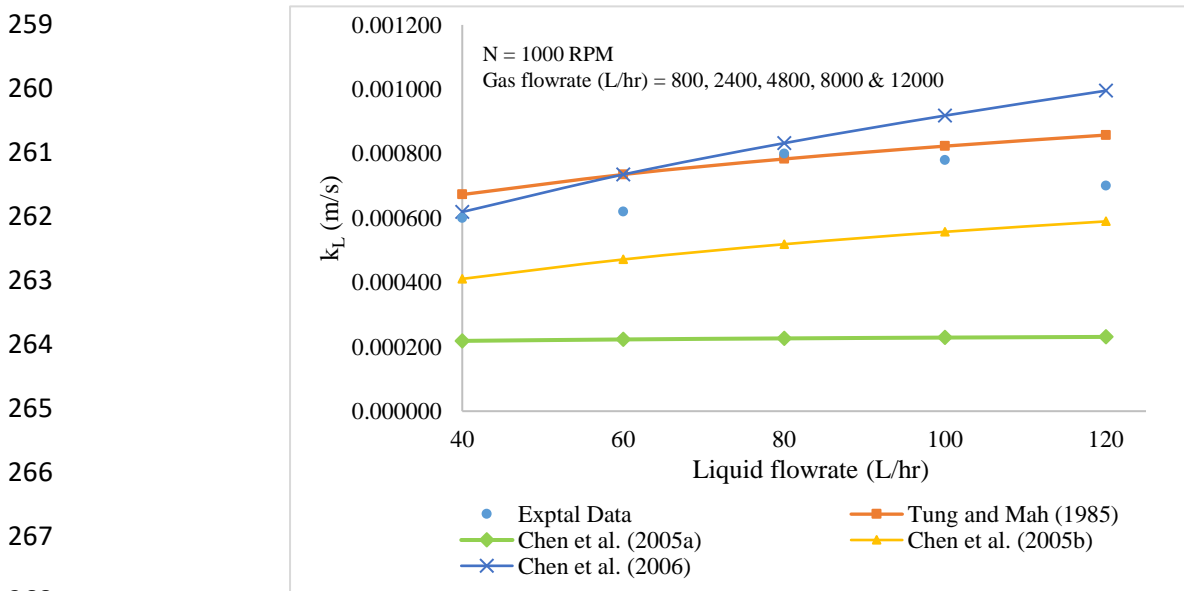
236 4.2 Results and discussion

237 The Luo et al (2012a) correlations for effective interfacial area, demonstrated in Case 1 to give good predictions
 238 for unsplit and unstructured wire mesh packing, was used to predict the effective interfacial area for all the cases.
 239 Although, this potentially increases the prediction uncertainty, the results (Figure 6 and 7) show a reasonably good

240 agreement for Tung and Mah (1985) and Chen et al. (2006). The results further showed that the predictions of
 241 Tung and Mah (1985), Chen et al. (2005a), Chen et al. (2005b) and Chen et al. (2006) correlations for liquid
 242 phase mass transfer coefficient were in the order of 10^{-4} . This is a typical range for liquid film mass transfer
 243 coefficients for RPBs which have been generally reported in the literature (Rao et al., 2004). The correlations of
 244 Onda et al. (1968) and Munjal et al. (1989a) respectively showed under-prediction and over-prediction in the
 245 orders of 10^{-5} and 10^{-3} at different rotating speed and liquid flowrate (Figures 8 and 9). The predictions of Onda
 246 et al. (1968) were in the typical range for the packed columns. It is concluded that modifying Onda et al. (1968)
 247 correlation by replacing the “g” term with “ $r\omega^2$ ” term do not result in good estimation of the liquid film mass
 248 transfer coefficient in RPBs.



258 Figure 6 Liquid film mass transfer coefficient at different RPM



269 Figure 7 Liquid film mass transfer coefficient at different liquid flowrate

270 Comparing the Chen correlations (Chen et al., 2005a; Chen et al., 2005b; Chen et al., 2006), Chen et al. (2006)
 271 gave the best prediction compared to others. This is because apparently more extensive data set that cover different
 272 packing types, fluid types (Newtonian and non-Newtonian) and radial depth were used to develop the correlation.
 273 The Chen et al. (2006) and Tung and Mah (1985) correlations gave the best prediction for all conditions. The
 274 performance of Tung and Mah (1985) is particularly interesting as it is simpler, requiring fewer parameters and
 275 most of all does not account for the end effect and the packing type. The predictions of Chen et al. (2006)

276 correlation, a supposedly more robust correlation that accounts for both end effect and packing type, tend to
 277 deviate as rotating speed and liquid flowrate increased. This deviation could be as a result of a combination of
 278 uncertainties from interfacial area and physical property predictions. Regardless, the maximum deviation was
 279 about 11% which is acceptable for most applications.

280

281

282

283

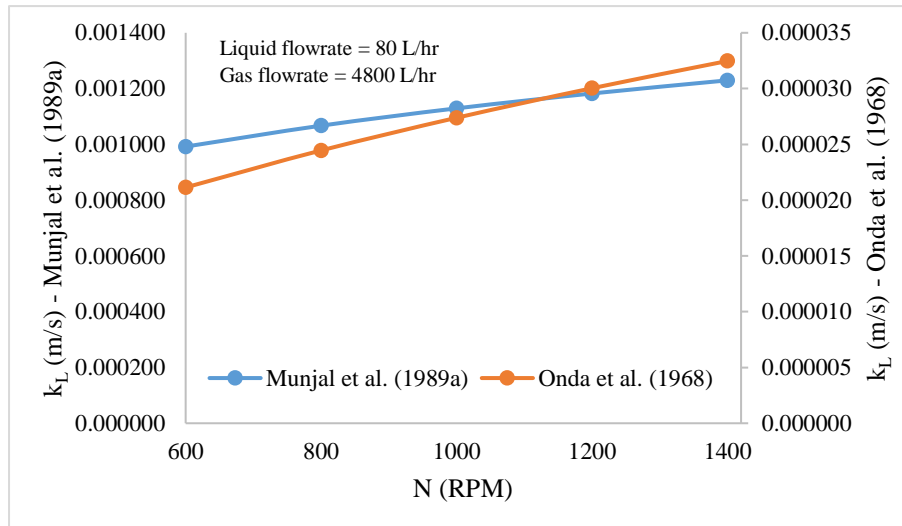
284

285

286

287

288



289

Figure 8 Liquid film mass transfer coefficient at different RPM

290

291

292

293

294

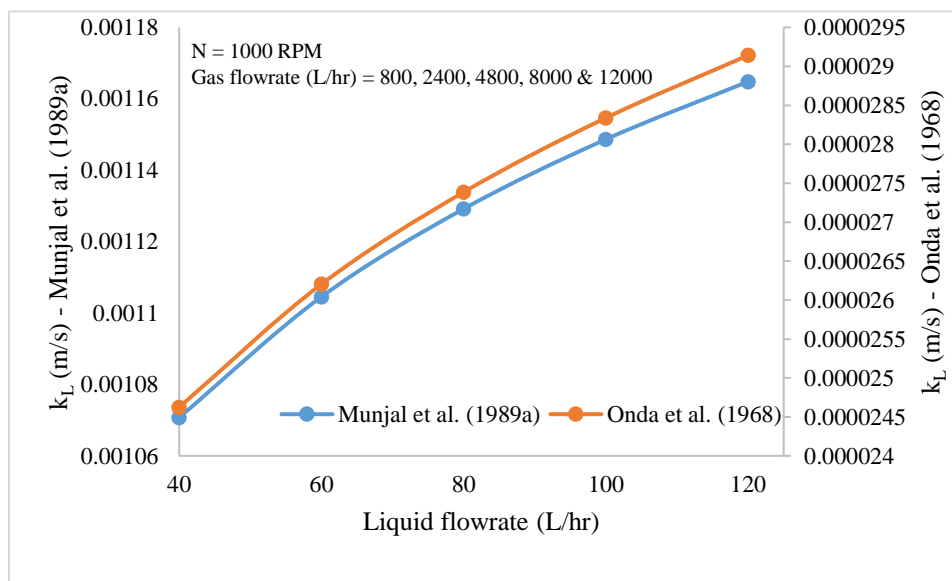
295

296

297

298

299



300

Figure 9 Liquid film mass transfer coefficient at different liquid flowrate

301

5. Case 3: Gas film mass transfer coefficient (k_G)

302

5.1 Experimental data and correlations

303

304 Experimental data for the gas film mass transfer coefficient (k_G) calculation for RPBs are not available in the
 305 literature. What have generally been reported are overall volumetric mass transfer coefficient (i.e. K_{GA}). The K_{GA}
 306 data are obtained using mass balance and the transfer unit concept (Liu et al., 1996; Chen and Liu, 2002; Lin et
 307 al., 2003; Lin et al., 2004; Chiang et al., 2009; Lin and Chu, 2015). The gas film volumetric mass transfer
 308 coefficient (i.e. $k_G a$) data have also been reported by Chen (2011). The $k_G a$ data from Chen (2011) was obtained
 309 based on the two-film theory (Eqn. 6) using a combination of published K_{GA} data and $k_L a$ data predicted using
 the Chen et al. (2006) correlation. In this study, a similar approach as Chen (2011) has been adopted to obtain gas

310 film mass transfer coefficient data (k_G) from published K_{GA} data alongside effective interfacial area and k_L data
 311 predicted using Luo et al. (2012a) and Tung and Mah (1985) correlations respectively. Two independent sources,
 312 namely Lin et al. (2004) and Chiang et al. (2009), for K_{GA} data were selected. The Lin et al. (2004) and Chiang
 313 et al. (2009) data involved isopropyl alcohol absorption in water and ethanol absorption in water respectively.
 314 Parameters of the RPB rigs used in both cases are summarized in Table 6.

315 Table 6 Specification of RPB from Lin et al. (2004) and Chiang et al. (2009)

	Dimensions (mm)				Packing		
	r_i	r_o	r_s	Z	Type	a_t	ϵ
Lin et al. (2004)	35	80	150	35	Wire mesh	791	0.96
Chiang et al. (2009)	20	40	60	20	Wire mesh	1024	0.944

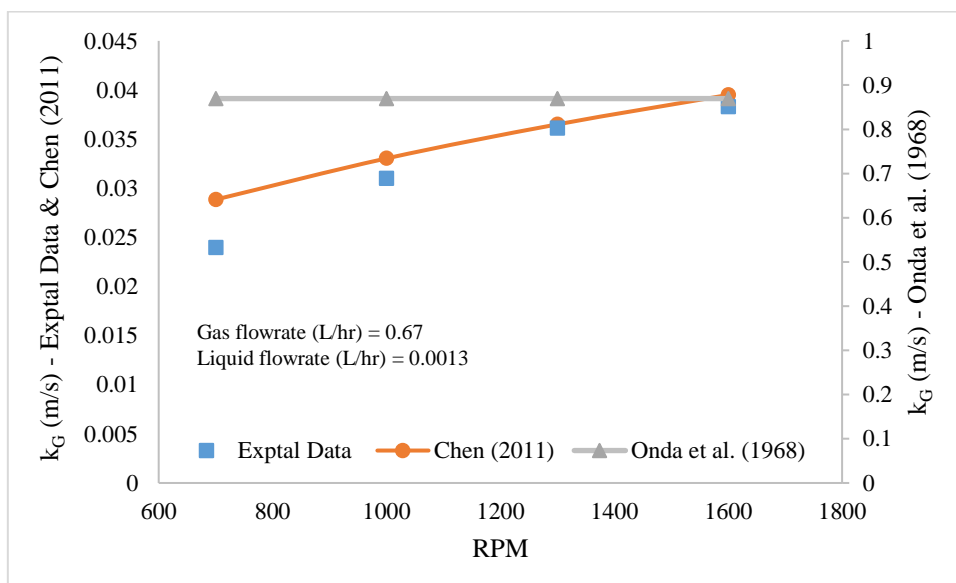
316
 317 Existing correlations for the gas-side mass transfer coefficients are presented in Table 7. The correlations of Lin
 318 et al. (2004), Liu et al. (1996) and Chen and Liu (2002) are formulated for predicting overall volumetric mass
 319 transfer coefficient (K_{GA}). The gas film mass transfer coefficient (k_G) can be calculated from these correlations
 320 using Eqn 6. This will involve predicting several parameters namely the Henry's constant, enhancement factor
 321 (where applicable), liquid film mass transfer coefficient, effective interfacial area and physical properties such as
 322 density, viscosity and surface tension. The uncertainties in predicting these parameters could result in significant
 323 error in the gas film mass transfer coefficient. Therefore it was concluded that the correlations proposed in Lin et
 324 al. (2004), Liu et al. (1996) and Chen and Liu (2002) are not good options for predicting the gas film mass transfer
 325 coefficient and was therefore not considered for validation in this study.

326 Table 7 Correlations for calculating gas-side mass transfer coefficient in RPBs

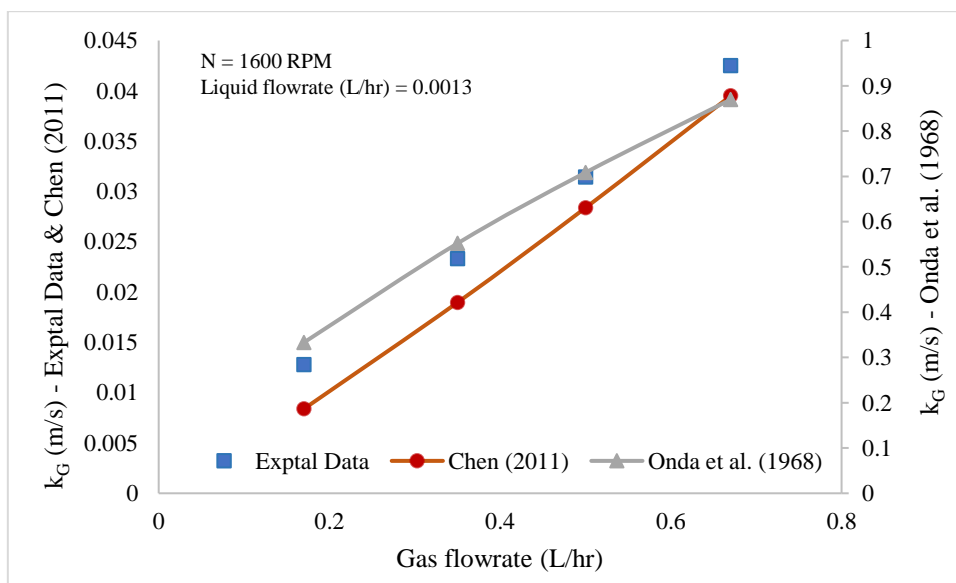
Correlations	Source	Comment
$\frac{k_G}{a_t D_G} = K_5 \left(\frac{V_m^*}{\mu_G a_t} \right)^{0.7} \left(\frac{\mu_G}{\rho_G D_G} \right)^{\frac{1}{3}} (a_t d_p)^{-2.0}$	Onda et al. (1968)	Correlation for predicting k_G in packed columns
$\frac{K_G a}{D_G a_t^2} = 3.11 \times 10^{-3} \left(\frac{V_m^*}{\mu_G a_t} \right)^{1.163} \left(\frac{L_m^*}{\mu_L a_t} \right)^{0.631} \left(\frac{d_p^3 \rho_G^2 r \omega^2}{\mu_G^2} \right)^{0.25}$	Liu et al. (1996)	These correlations are developed for predicting $K_G a$ in RPBs. The k_G can then be derived from the predicted $K_G a$ data using Eqn 6.
$\frac{K_G a H^{0.27}}{D_G a_t^2} = 0.077 \left(\frac{V_m^*}{\mu_G a_t} \right)^{0.323} \left(\frac{L_m^*}{\mu_L a_t} \right)^{0.328} \left(\frac{d_p^3 \rho_G^2 r \omega^2}{\mu_G^2} \right)^{0.18}$	Chen and Liu (2002)	
$\frac{K_G a H^{0.315}}{D_G a_t^2} = 0.061 \left(\frac{V_m^*}{\mu_G a_t} \right)^{0.712} \left(\frac{L_m^*}{\mu_L a_t} \right)^{0.507} \left(\frac{d_p^3 \rho_G^2 r \omega^2}{\mu_G^2} \right)^{0.326}$	Lin et al. (2004)	
$\frac{k_G a}{D_G a_t^2} V_G = K_n \left(\frac{V_m^*}{\mu_G a_t} \right)^{1.13} \left(\frac{L_m^*}{\mu_L a_t} \right)^{0.14} \left(\frac{d_p^3 \rho_G^2 r \omega^2}{\mu_G^2} \right)^{0.31} \left(\frac{L_m^{2*}}{\sigma_L \rho_L a_t} \right)^{0.07} \left(\frac{a_t}{a_p} \right)^{1.4}$	Chen (2011)	The correlation is developed for predicting $k_G a$ in RPBs

327
 328 Mukherjee et al. (2001) and Sandilya et al. (2001) had suggested that the gas phase undergoes a 'solid-body'-like
 329 rotation within the rotor of an RPB because of the drag offered by the packing and as a result suggested there was
 330 no enhancement of the gas film volumetric mass transfer resistance (k_{GA}). Consequently, they concluded that the
 331 gas film volumetric mass transfer coefficient in RPBs was in similar range as that of packed columns. This was
 332 further demonstrated in Chen and Liu (2002) where it was shown that enhancements in k_{GA} are mainly attributed
 333 to the interfacial area (a), while k_G remain in similar range as that of the packed columns. These conclusions have
 334 prompted the use of Onda et al. (1968) for predicting the gas film mass transfer coefficient in most published
 335 studies of RPBs (Joel et al., 2014; Kang et al., 2014). As a result, Onda et al. (1968) correlation for gas-film mass
 336 transfer coefficient was also evaluated in this study.

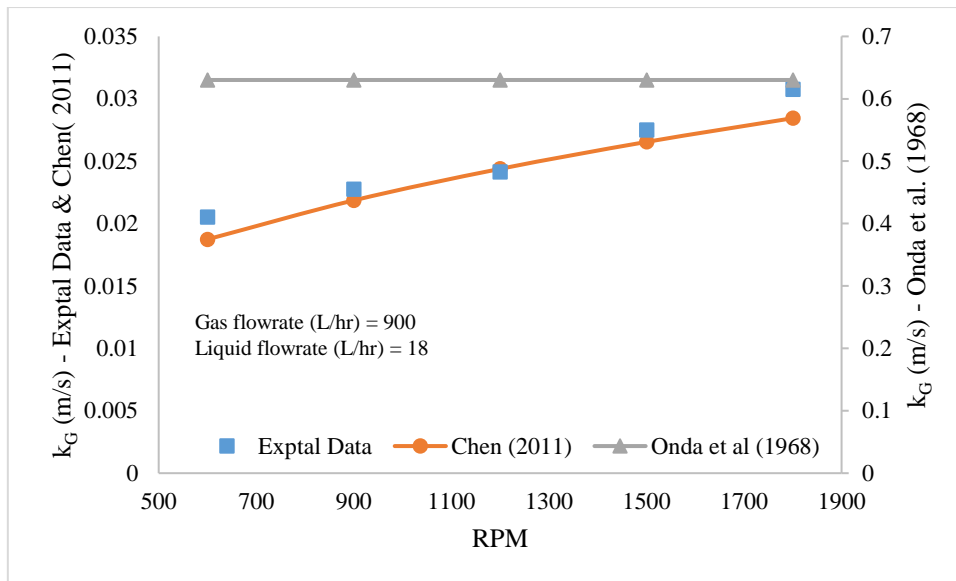
338 The results of comparison between predicted values and experimental data (Figures 10 and 11) show that for the
 339 two experimental data considered in this study (Lin et al., 2004; Chiang et al., 2009), the Onda et al. (1968)
 340 correlation significantly over-predicts the k_G in the RPBs for different rotating speed and gas flowrate. The
 341 predictions of Onda et al. (1968) are in the order of 10^{-1} in contrast to order of 10^{-2} values for the experimental
 342 data. Predictions of Chen (2011) on the other hand were in the order of 10^{-3} . With the parameter K_n updated from
 343 0.023 to 0.23, there was good agreement between the predictions of Chen (2011) and the experimental data for
 344 the two independent data sources in this study. Onda et al. (1968) correlation do not have a “g” term and as such
 345 they do not show the influence of centrifugal acceleration when they are used for predicting the k_G in RPBs (Figure
 346 10a and 11a). The experimental data as well as predictions of Chen (2011) both show that rotation enhances gas
 347 side resistance. Figures 10a and 11a both show that increasing rotating speed from 700-1600 RPM (Lin et al.,
 348 2004) and 600-1800 RPM (Chiang et al., 2009) respectively will enhance gas side resistance by up to 30%. While
 349 k_G appears to be in similar range as that of packed columns in agreement with the conclusions reached in
 350 Mukherjee et al. (2001) and Sandilya et al. (2001), their actual values are however affected by rotating speed. It
 351 is not possible to capture this impact when k_G in RPBs are predicted using Onda et al. (1968).



352
 353 Figure 10a Comparisons to experimental data from Lin et al. (2004) data



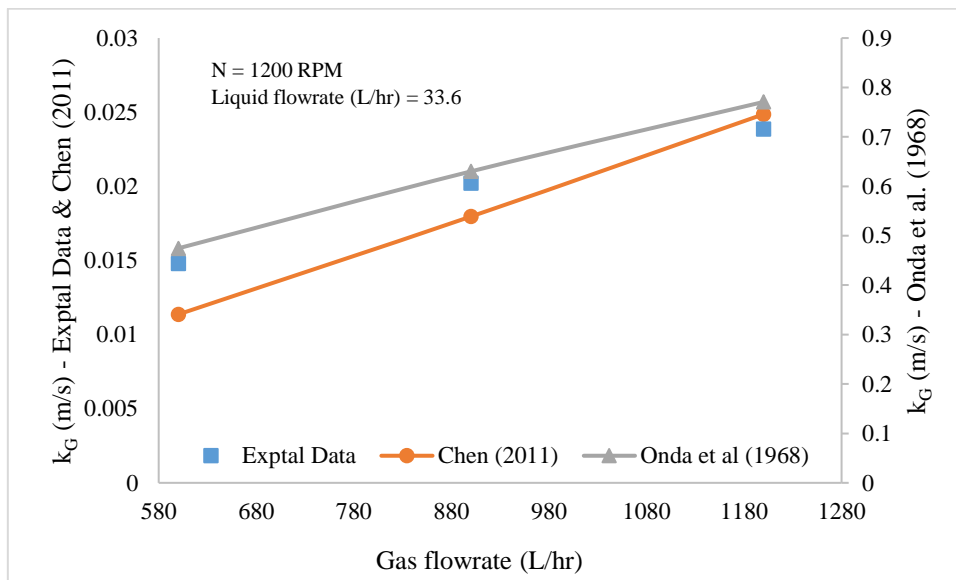
354
 355 Figure 10b Comparisons to experimental data from Lin et al. (2004) data



356

357

Figure 11a Comparisons to Chiang et al. (2009) data



358

359

Figure 11a Comparisons to Chiang et al. (2009) data

360 6. Conclusions and recommendations for future study

361 The RPB is a promising technology that can greatly reduce the size and cost of packed columns used for absorption
 362 and desorption in solvent-based CO₂ capture and natural gas treating processes. Mass transfer prediction in RPBs
 363 is not sufficiently proven because necessary correlations for doing this are generally few in literature and the
 364 prediction accuracy for existing correlations have not been demonstrated independently. In this study, an RPB
 365 model was developed in gPROMS ModelBuilder® and used to test and compare different correlations for the
 366 effective interfacial area, the liquid and gas film mass transfer coefficients at different rotating speed and liquid/gas
 367 flowrate. The results presented in this paper show that modified packed column mass transfer correlations with
 368 the “g” term (i.e. gravitational acceleration) replaced with “rw²” (i.e. centrifugal acceleration) commonly used in
 369 literature for RPBs generally give poor predictions. The Tung and Mah (1985) correlation gave a good prediction
 370 of liquid film mass transfer coefficient in RPBs, slightly better than more complex correlations such as the Chen
 371 et al. (2006). The data of gas film mass transfer coefficient for RPBs were also derived from overall mass transfer
 372 coefficient ($K_G a$) experimental data from the literature. This is the first report of gas film mass transfer data for
 373 RPBs in literature. Finally, we demonstrated that Chen (2011) predicts gas film mass transfer coefficient better

374 when the parameter (K_n) is updated from 0.023 to 0.23 comparing against two independent data. The validity of
375 the analysis and conclusions in this study are based on a single type of packing (unstructured wire mesh). With
376 other packing types, namely expamet and retimet among others, the performance of the correlations may be very
377 different. For instance, efforts in our group to use Luo et al. (2012a) for predicting effective interfacial area of
378 expamet packings showed that the predicted values were out of range, although more data is needed to confirm
379 this finding. The performance of the correlations should be demonstrated for other types of packings for RPB such
380 as expamet and retimet as the relevant data become available.

381 Acknowledgements

382 The authors are grateful to the UK Engineering and Physical Sciences Research Council (EPSRC) (Ref:
383 EP/M001458/2 and EP/N024672/1) for financing this research.

384 References

- 385 Agarwal, L., Pavani, V., Rao, D. and Kaistha, N. 2010. Process intensification in HiGee absorption and
386 distillation: design procedure and applications. *Ind Eng. Chem Res*, 49, 46–58.
- 387 Chambers, H.H. and Wall, R.G. 1954. Some factors affecting the design of centrifugal gas absorbers. *Trans*
388 *Instn Chem Engrs* 32, 96-107.
- 389 Chen, Y.-S., Lin, F.-Y., Lin, C.-C., Tai, C. Y.-D., and Liu, H.-S. 2006. Packing characteristics for mass transfer in
390 a rotating packed bed. *Ind. Eng. Chem. Res.*, 45, 6846–6853.
- 391 Chen, Y.-S. 2011. Correlations of mass transfer coefficients in a rotating packed bed. *Ind. Eng. Chem. Res.*, 50,
392 1778–1785.
- 393 Chen, Y. S., Lin, C. C. and Liu, H.S. 2005a. Mass transfer in a rotating packed bed with viscous newtonian and
394 non-newtonian fluids. *Ind. Eng. Chem. Res.*, 44, 1043-1051.
- 395 Chen, Y. S. Lin, C. C. and Liu, H.S. 2005b. Mass transfer in a rotating packed bed with various radii of the bed.
396 *Ind. Eng. Chem. Res.*, 44, 7868- 7875.
- 397 Chen, H.H., Deng, X.H., Zhang, J.J. and Zhang, Y.J. 1999. The effective gas–liquid interfacial area and
398 volumetric mass-transfer coefficient measured by chemical absorption method in rotating packed bed with
399 multiple spraying under centrifugal force, *Chem. React. Eng. Technol.* 15, 97–103 (in Chinese).
- 400 Chen, H.H., Jian, Q.F. and Deng, X.H. 1997. The measurement of effective gas–liquid interfacial area of
401 rotating bed by chemical absorption method, *J. South China Univ. Technol.* 27, 32–37 (in Chinese).
- 402 Chen, Y. S. and Liu, H.S. 2002. Absorption of VOCs in a rotating packed bed. *Ind. Eng. Chem. Res.*, 41, 1583-
403 1588.
- 404 Chen, Y.-S, Hsu, Y.-C, Lin, C.-C, Tai, C.Y.-D and Liu H.-S. 2008. Volatile organic compounds absorption in a
405 cross-flow rotating packed bed. *Environ Sci Technol* 42, 2631–2636.
- 406 Chiang, C.-Y., Chen, Y.-S., Liang, M.-S., Lin, F.-Y. & Tai, C. Y.-D. and Liu, H.-S. 2009. Absorption of ethanol
407 into water and glycerol/water solution in a rotating packed bed. *Journal of the Taiwan Institute of*
408 *Chemical Engineers*, 40, 418–423.
- 409 Chu, G.-W., Sang, L., Du, X.-K., Luo, Y., Zou, H.-K., Chen, J.-F. 2015. Studies of CO₂ absorption and effective
410 interfacial area in a two-stage rotating packed bed with nickel foam packing. *Chem. Eng. Process.* 90, 34–
411 40.
- 412 Ding, X., Hu, X., Ding, Y., Wu, Y. and Li, D. 2000. A model for the mass transfer coefficient in rotating packed
413 bed. *Chem. Eng. Cam.*, 178, 249–256.
- 414 Florin, N. and Fennell, P. n.d. Assessment of the validity of “approximate minimum land footprint for some
415 types of CO₂ capture plant” provided as a guide to the Environment Agency assessment of carbon capture
416 readiness in DECC’s CCR Guide for Application under Section 36 of the Electricity Act 1989.
- 417 Garcia, G.E.C., van der Schaaf, J. and Kiss, A.A. 2017. A review on process intensification in HiGee
418 distillation. *J Chem Technol Biotechnol.*, 92, 1136-1156.
- 419 Guo, K., Zhang, Z., Luo, H., Dang, J. and Qian, Z. 2014. An innovative approach of the effective mass transfer
420 area in the rotating packed bed. *Ind. Eng. Chem. Res.*, 53, 4052–4058.
- 421 Guo, F., Zheng, C., Guo, K., Feng, Y. and Gardner, N.C 1997. Hydrodynamics and mass transfer in cross-flow
422 rotating packed bed. *Chem Eng. Sci.*, 52, 3853–3859.
- 423 HiGee 2014. Available at: <http://higeeusa.com/H2S.html> [Accessed Dec., 2018].
- 424 IEAGHG, “Post-combustion CO₂ capture scale-up study”, 2013/05, February, 2013.

425 Jassim, M.S., Rochelle, G., Eimer, D., Ramshaw, C. 2007. Carbon dioxide absorption and desorption in aqueous
426 monoethanolamine solutions in a rotating packed bed. *Ind. Eng. Chem. Res.*, 46, 2823–2833.

427 Joel, A. S., Wang, M., Ramshaw, C., Oko, E. 2014. Process analysis of intensified absorber for post-combustion
428 CO₂ capture through modelling and simulation. *Journal of Greenhouse Gas Control*, 21, 91–100.

429 Kang, J.-L., Sun, K., Wong, D. S.-H., Jang, S.-S., and Tan, C.-S. 2014. Modelling studies on absorption of CO₂
430 by monoethanolamine in rotating packed bed. *International Journal of Greenhouse Gas Control*, 25, 141–
431 150.

432 Kolawole, T., Attidekou, P., Hendry, J. and Lee, J. Comparative study of CO₂ capture using counter and cross
433 flow configurations in a rotating packed bed absorber using monoethanolamine (MEA). 14th International
434 Conference on Greenhouse Gas Control Technologie (GHGT-14), October 21 -25, 2018, Melbourne,
435 Australia.

436 Lawal, A., Wang, M., Stephenson, P. and Obi, O. 2012. Demonstrating full-scale post-combustion CO₂ capture
437 for coal-fired power plants through dynamic modelling and simulation. *Fuel*, 101, 115–128.

438 Lin, C.-C. and Liu, W.-T., 2007. Mass transfer characteristics of a high-voidage rotating packed bed. *J. Ind.*
439 *Eng. Chem.*, 13(1), 71–78.

440 Lin, C.-C., Chen, Y.-S. and Liu, H.-S. 2000. Prediction of liquid holdup in countercurrent-flow rotating packed
441 bed. *Trans IChemE*, Vol. 78, Part A, 397-403.

442 Lin, C. C., Wei, T. Y., Liu, W. T. and Shen, K.P. 2004. Removal of VOCs from gaseous streams in a high-
443 voidage rotating packed bed. *J. Chem. Eng. Jpn.*, 37, 1471-1477

444 Lin, C.-C., Liu, W.-T. and Tan, C.-S., 2003. Removal of Carbon Dioxide by Absorption in a Rotating Packed
445 Bed. *Ind. Eng. Chem. Res.*, 42, 2381–2386.

446 Lin, C.-C. and Chu, C.-R., 2015. Mass transfer performance of rotating packed beds with blade packings in
447 carbon dioxide absorption into sodium hydroxide solution. *Separation and Purification Technology*, 150,
448 196–203.

449 Liu, Y., Gu, D., Xu, C., Qi, G. and Jiao, W. 2015. Mass transfer characteristics in a rotating packed bed with
450 split packing. *Chinese Journal of Chemical Engineering*, 23, 868–872

451 Liu, H.-S., Lin, C.-C., Wu, S.-C. and Hsu, H.-W., 1996. Characteristics of a rotating packed bed. *Ind. Eng.*
452 *Chem. Res.*, 35, 3590–3596.

453 Luo, Y., Chu, G.W., Zou, H.K. Zhao, Z.Q., Dudukovic, M.P. and Chen, J.F. 2012a. Gas–liquid effective
454 interfacial area in a rotating packed bed. *Ind. Eng. Chem. Res.*, 51, 16320–16325.

455 Luo, Y., Chu, G.-W., Zou, H.-K., Wang, F., Xiang, Y., Shao, L. and Chen, J.-F. 2012b. Mass transfer studies in
456 a rotating packed bed with novel rotors: Chemisorption of CO₂. *Ind. Eng. Chem. Res.*, 51, 9164–9172.

457 Luo, Y., Luo, J.-Z., Chu, G.-W., Zhao, Z.-Q., Arowo, M. and Chen, J.-F. 2017. Investigation of effective
458 interfacial area in a rotating packed bed with structured stainless steel wire mesh packing. *Chemical*
459 *Engineering Science* 170, 347-354.

460 Mukherjee, R., Deb, D., Sandilya, P. and Rao, D.P., 2001. Gas-phase mass transfer in a centrifugal gas-liquid
461 contactor with a stack of flexible disks as packing. In: Regel, L. L. and Wilcox, W. R. (eds) *Processing by*
462 *centrifugation*. Boston, Massachusetts: Springer, 51–60.

463 Munjal, S., Dudukovic, M. P. and Ramachandran, P. 1989a. Mass-transfer in rotating packed beds-I:
464 Development of gas-liquid and liquid-solid mass-transfer correlations. *Chem. Eng. Sci.*, 44, 2245- 2256.

465 Munjal, S., Dudukovic, M. P. and Ramachandran, P., 1989b. Mass transfer in rotating packed beds-II.
466 Experimental results and comparison with theory and gravity flow. *Chemical Engineering Science*,
467 44(10), 2257–2268.

468 Nascimento, J. V. S., Ravagnani, T. M. K. and Pereira, J. A. F. R. 2009. Experimental study of a rotating packed
469 bed distillation column. *Brazilian Journal of Chemical Engineering*, 26(1), 219-226.

470 Oko, E. 2015. Study of power plant, carbon capture and transport network through dynamic modelling and
471 simulation. PhD Thesis, School of Engineering, University of Hull.

472 Oko, E., Ramshaw, C. and Wang, M. 2018. Study of intercooling for rotating packed bed absorbers in
473 intensified solvent-based CO₂ capture process. *Applied Energy* 223 (2018), 302-316.

474 Rajan, S., Kumar, M., Ansari, M. J., Rao, D. P. and Kaistha, N., 2011. Limiting gas liquid flows and mass
475 transfer in a novel rotating packed bed (HiGee). *Ind. Eng. Chem. Res.*, 50, 986–997.

476 Rajan, S., Kumar, M., Ansari, M. J., Rao, D. P. and Kaistha, N., 2011. Limiting gas liquid flows and mass
477 transfer in a novel rotating packed bed (HiGee). *Ind. Eng. Chem. Res.*, 50, 986–997.

478 Ramshaw, C. and Mallinson, R.H. 1981. Mass Transfer Process. US Patent: 4283255

- 479 Rao, D. P., Bhowal, A. and Goswami, P.S. 2004. Process intensification in rotating packed beds (HIGEE): An
480 appraisal. *Ind. Eng. Chem. Res.*, 43, 1150–1162.
- 481 Sandilya, P., Rao, D. P. Sharma, A. and Biswas, G., 2001. Gas-phase mass transfer in a centrifugal contactor.
482 *Ind. Eng. Chem. Res.*, 40, 384–392.
- 483 Thiels, M., Wong, D. S. H., Yu, C.-H., Kang, J.-L., Jang, S. S., Tan, C.-S. 2016. Modelling and design of carbon
484 dioxide absorption in rotating packed bed and packed column. In 11th IFAC Symposium on Dynamics and
485 Control of Process Systems, including Biosystems. Trondheim, Norway.
- 486 Tsai, C.-Y. and Chen, Y.-S. 2015. Effective interfacial area and liquid-side mass transfer coefficients in a
487 rotating bed equipped with baffles. *Separation and Purification Technology* 144, 139–145.
- 488 Tung, H. H.; Mah, R.S.H. 1985. Modeling liquid mass transfer in Hige separation process. *Chem. Eng.*
489 *Commun.*, 39, 147-153.
- 490 Yang, K., Chu, G., Zou, H., Sun, B., Shao, L. and Chen, J.-F., 2011. Determination of the effective interfacial
491 area in rotating packed bed. *Chemical Engineering Journal*, 168, 1377–1382.
- 492 Ying, J. and Eimer, D. A. 2013. Determination and measurements of mass transfer kinetics of CO₂ in
493 concentrated aqueous monoethanolamine solutions by a stirred cell. *Ind. Eng. Chem. Res.* 52, 2548–2559.
- 494
- 495